

Supporting Information

Fabrication and characterization of high-tensile-strength PEO-PVP blend based multifunctional composites for sodium-ion structural batteries

Vasan Iyer*,^{1,2}, Sandeep Kumar³, Håkan Pettersson^{4,5}, Jan Petersen^{1,2}, Sebastian Geier^{1,2}, and Peter Wierach^{1,2,6}

¹Cluster of Excellence SE2A - Sustainable and Energy Efficient Aviation, Technische Universität Braunschweig, 38108, Braunschweig, Germany

²Institute of Lightweight Systems, Department of Multifunctional Materials, German Aerospace Center (DLR), Lilienthalplatz 7, 38108, Braunschweig, Germany

³Center for Nanoscience and Nanotechnology, Jamia Millia Islamia, New Delhi, 110025, India

⁴School of Information Technology, Halmstad University, Box 823, SE-301 18 Halmstad, Sweden

⁵Solid State Physics and NanoLund, Lund University, Box 118, SE-221 00 Lund, Sweden

⁶Institute of Polymer Materials and Plastics Engineering, Technische Universität Clausthal, Agricolastrasse 6, Clausthal-Zellerfeld, 38678, Germany

*Corresponding author, E-mail: vasan.iyer@dlr.de, vasan.iyer@tu-clausthal.de

Table of Contents

1.	EXPERIMENTAL SECTION.....	S4
1.1.	Chemicals and materials.....	S4
1.2.	Synthesis of InAs nanowires.....	S5
1.3.	Preparation of Pure Sodium Metal Foils	S6
2.	SUPPLEMENTARY INFORMATION FIGURES.....	S7
3.	REFERENCES.....	S19

List of Figures and Tables

Figure S1. (a) Schematic showing the synthesis of InAs nanowires.	5
Figure S2. 2032-coin cell configuration for: (a) Symmetrical cell. (b) Asymmetrical cell.....	7
Figure S3. a) Experimental set-up for precise elongation measurements using ZEISS ARAMIS 3D industrial camera. b) Tensile test experiment set-up with sample in the universal testing machine (UTM) (using Zwick GmbH & Co. KG, Ulm, Germany).	7
Figure S4. 2032-coin cell configuration for structural battery half-cell.	8
Figure S5. XRD spectrum of InAs nanowires.	8
Figure S6. Figure S6. SEM image showing uniform distribution of InAs nanowires on the surface of structural electrolyte GF_PEO-PVP-InAsNW-NaPF ₆ ,	9
Figure S7. (a) EDAX pattern for the structural electrolyte GF_PEO-PVP-InAsNW-NaPF ₆ . (b) SEM-EDAX element mapping for the structural electrolyte.....	10
Figure S8. Fabricated electrolytes samples: (a) SPE PEO-PVP-NaPF ₆ . (b) SPE PEO-PVP-InAsNW-NaPF ₆ . (c) Structural electrolyte GF_PEO-PVP-NaPF ₆ . (d) Structural electrolyte GF_PEO-PVP-InAsNW-NaPF ₆ . (e) Structural electrode upper surface. (f) Structural electrode lower surface showing intermediate carbon fiber electrode	11
Figure S9. Electrochemical impedance spectroscopy (EIS) equivalent circuit for the electrolytes, with Cdl - the double layer interface capacitance, and W – Warburg element representing the solid-state diffusion of Na ⁺ into the electrodes.	11
Figure S10. Electrochemical impedance spectroscopy (EIS) spectra of solid polymer electrolytes filled with various amounts of InAs nanowires plotted on double logarithmic scale. ³	12
Figure S11. Ionic conductivities of electrolytes at different temperatures.	12

Figure S12. EIS spectra before and after dc polarization for transference-ion measurements: a) Na PEO-PVP-NaPF ₆ Na. b) Na GF_PEO-PVP-InAsNW-NaPF ₆ Na.....	13
Figure S13. Samples for tensile testing prepared according to ASTM D-638 standards: (a) SPE PEO-PVP-NaPF ₆ . (b) SPE PEO-PVP-InAsNW-NaPF ₆ . (c) Structural electrolyte GF_PEO-PVP-InAsNW-NaPF ₆ . (d) Structural electrode CF GF_PEO-PVP-InAsNW-NaPF ₆	13
Figure S14. Plot showing comparison of the tensile strength of structural electrolytes for sodium-ion based structural battery.....	14
Figure S15. Statistical analysis of tensile tests for: (a) Solid polymer electrolytes. (b) Structural electrolyte and structural electrode.....	15
Figure S16. Force – displacement plots from tensile testing: (a) SPE PEO-PVP-NaPF ₆ . (b) SPE PEO-PVP-InAsNW-NaPF ₆ . (c) Structural electrolyte GF_PEO-PVP-InAsNW-NaPF ₆ . (d) Structural electrode CF GF_PEO-PVP-InAsNW-NaPF ₆	15
Figure S17. Thermal stability tests: (a) SPE PEO-PVP-InAsNW-NaPF ₆ at 25°C. (b) Structural electrolyte GF_PEO-PVP-InAsNW-NaPF ₆ at 25°C. (c) SPE PEO-PVP-InAsNW-NaPF ₆ after heating to 160°C for 10 minutes. (d) Structural electrolyte GF_PEO-PVP-InAsNW-NaPF ₆ after heating to 160°C for 15 minutes.....	16
Figure S18. Plot showing comparison of energy density vs elastic modulus for various reported structural batteries in the literature [8, 10]. The plot also indicates the targets for structural batteries for aero applications for the year 2030+ (pink area). The grey area denotes the state-of-the-Art (SotA) for Li-ion batteries. Image reproduced with permission [11].	17
Figure S19. Plot showing comparison of the energy densities reported in different approaches for sodium-ion based structural cell.	17
Figure S20. Comparison of energy density vs elastic modulus for DOI III type structural batteries reported in literature.	18
Figure S21. SEM image of Na electrode of the structural cell CF PEO-PVP-InAsNW-NaPF6 Na after cycling.....	19
Table S1: Sodium-ion transference number calculations	S13
Table S2: Tensile strength comparison of solid polymer electrolytes.....	S14
Table S3. Table showing the performance comparison of various DOI III type structural batteries architectures reported in literature	S18

1. EXPERIMENTAL SECTION

1.1. Chemicals and materials.

Chemicals and materials for the synthesis of a structural electrolyte includes poly(ethylene oxide) (PEO with a molecular weight $M_w = 10^6$ g mol⁻¹), poly(vinyl pyrrolidone) (PVP with a molecular weight $M_w = 40000$ g mol⁻¹), methanol (CH₃OH), and sodium hexafluorophosphate (NaPF₆ with $M_w = 167.95$ g mol⁻¹) were purchased from Sigma-Aldrich, Steinheim, Germany). High purity chemicals and materials for the synthesis of InAs nanowires including Indium trichloride tetrahydrate (InCl₃.4H₂O), arsenic oxide (As₂O₃), polyethylene glycol (PEG) and ethylene glycol (EG), sodium borohydride (NaBH₄) and ethylenediamine (C₂H₄(NH₂)₂) were purchased from Sigma-Aldrich. Glass fiber woven fabric with aerial weight 163 g m⁻² and spread tow carbon fibers (CF) Tenax IMS65 24k tows with aerial weight 55 g m⁻² for the preparation of structural electrolyte and structural battery half-cell were purchased from R&G Faserverbundwerkstoffe GmbH, Waldenbuch, Germany. Pure sodium metal sticks for structural battery counter electrode were purchased from Alfa Aesar GmbH, Karlsruhe, Germany. Two-sided siliconized papers for heat press were obtained from Laufenberg GmbH, Krefeld, Germany.

1.2. Synthesis of InAs nanowires.

Figure 3a illustrates the InAs NW synthesis where indium trichloride tetrahydrate ($\text{InCl}_3 \cdot 4\text{H}_2\text{O}$) and arsenic oxide (As_2O_3) were used as reactants.

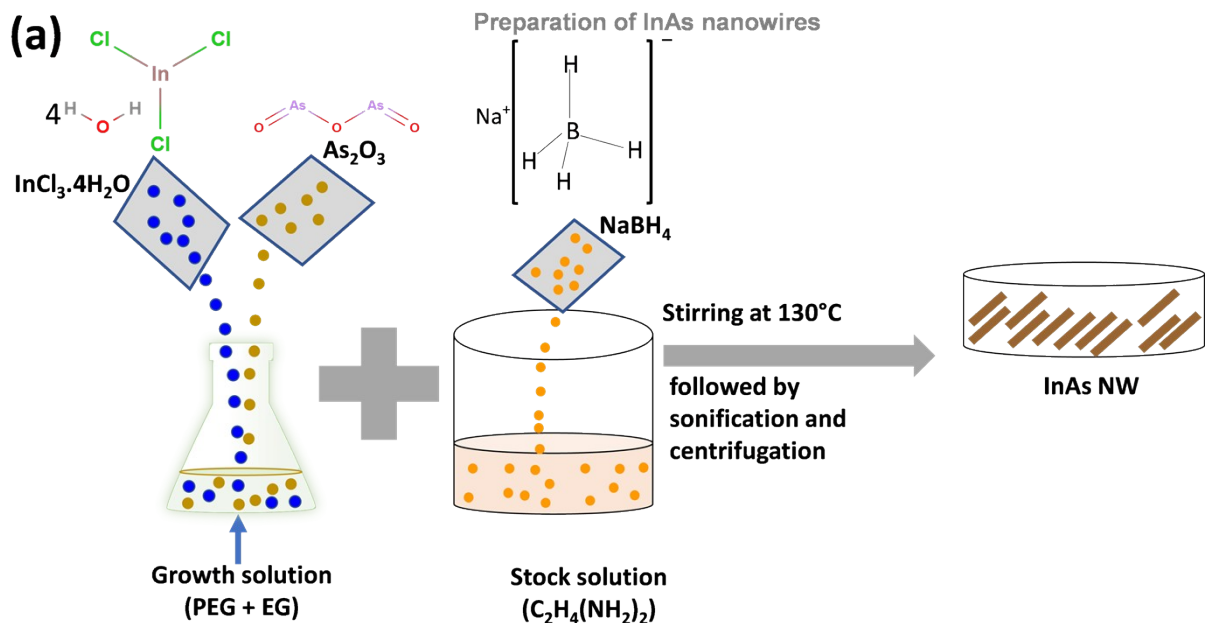


Figure S1. (a) Schematic showing the synthesis of InAs nanowires.

Polyethylene glycol (PEG) and ethylene glycol (EG) were used as solvents. In the growth step of InAs NWs, $\text{InCl}_3 \cdot 4\text{H}_2\text{O}$ and As_2O_3 were used as the source for indium (In) and arsenic (As) respectively, which were mixed in the solvent containing a mixture of PEG and EG to get the growth solution. The mixture is continuously stirred and heated at 130°C for 30 minutes and subsequently mixed with the stock solution (obtained by dissolving sodium borohydride in ethylenediamine) and was allowed to react for 1 hour. The combined mixture was sonicated and centrifuged and finally vacuum dried to obtain high quality InAs NWs.

1.3. Preparation of Pure Sodium Metal Foils.

The pure sodium metal foils are prepared inside the glove box in a protective atmosphere (with humidity of 0 ppm and oxygen of 0 ppm). The oil-coated oxidized layer of the sodium sticks is firstly removed and then the shiny sodium metal underneath is then cut and cleaned briefly with hexane solution and then immediately dried. The obtained sodium portion is then made into thin foils using a roller and finally cut into disc shape, as per coin cell requirements.

2. SUPPLEMENTARY INFORMATION FIGURES

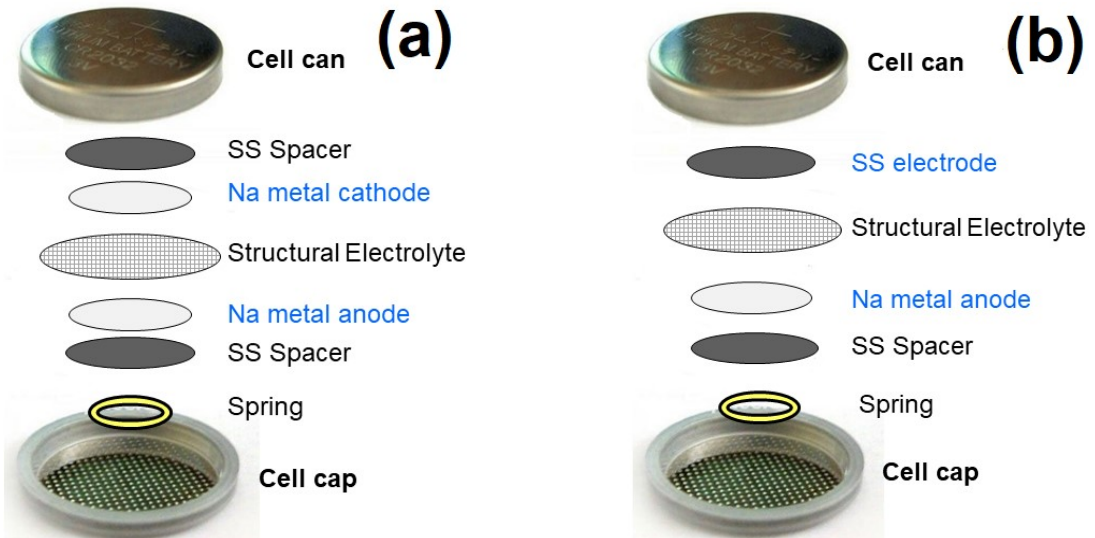


Figure S2. 2032-coin cell configuration for: (a) Symmetrical cell. (b) Asymmetrical cell.

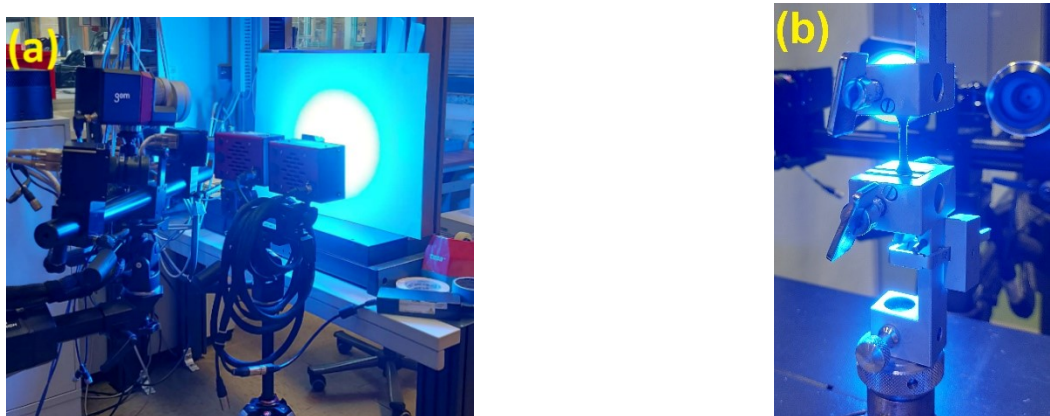


Figure S3. a) Experimental set-up for precise elongation measurements using ZEISS ARAMIS 3D industrial camera. b) Tensile test experiment set-up with sample in the universal testing machine (UTM) (using Zwick GmbH & Co. KG, Ulm, Germany).

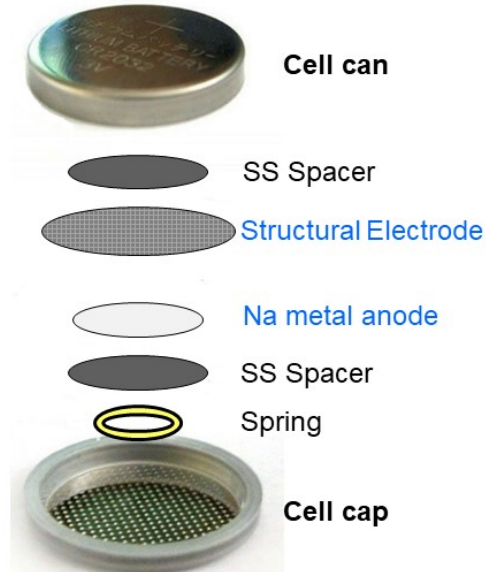


Figure S4. 2032-coin cell configuration for structural battery half-cell.

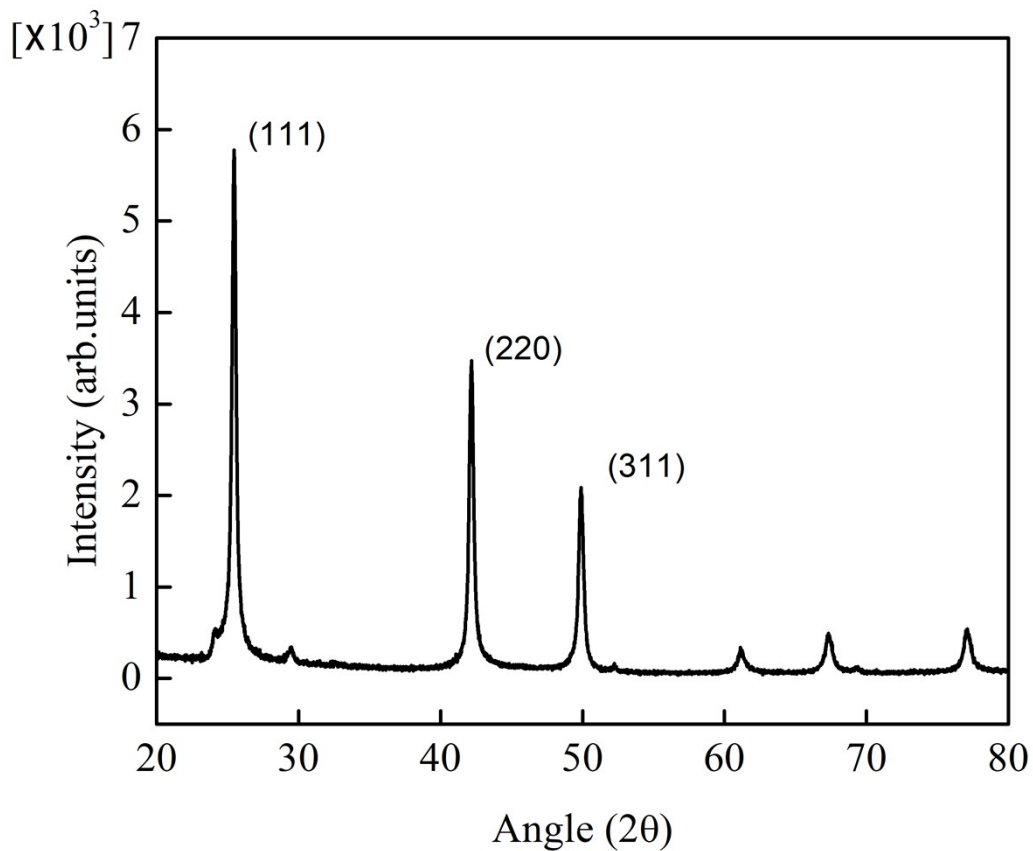


Figure S5. XRD spectrum of InAs nanowires.

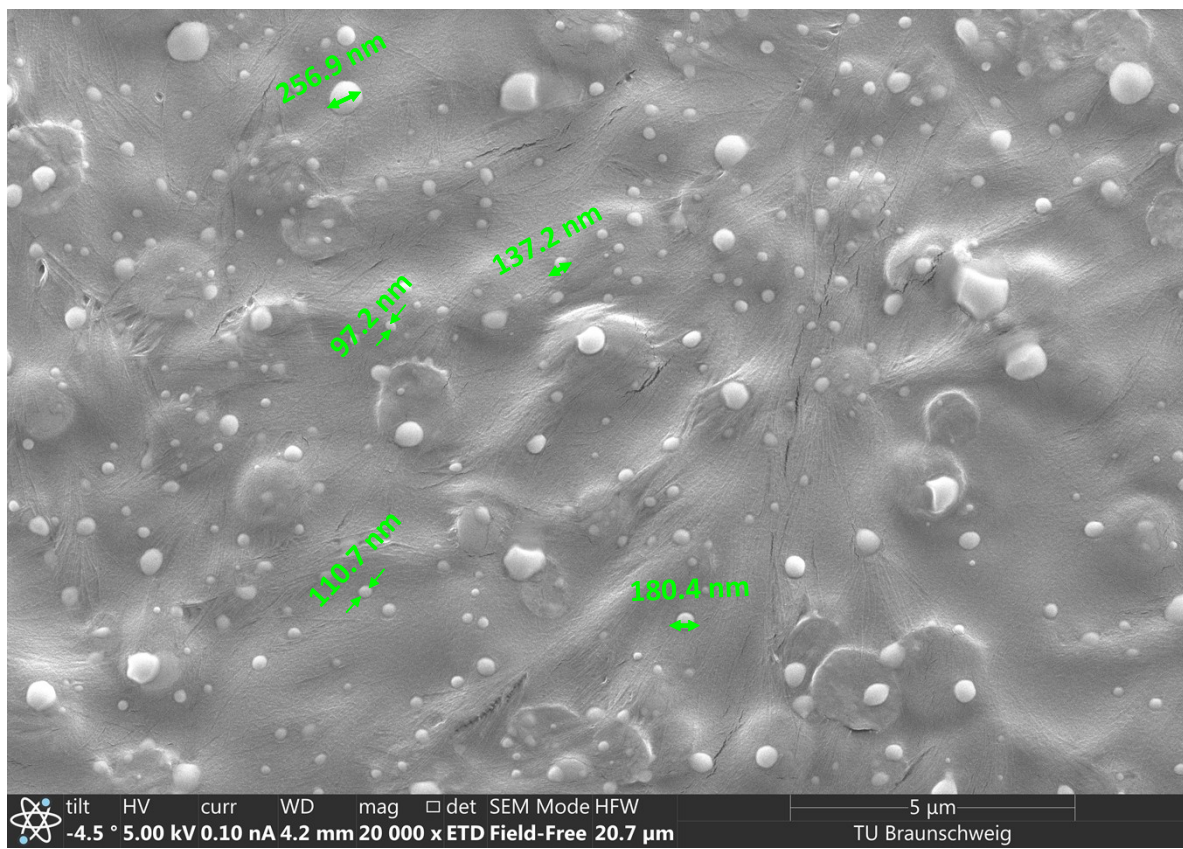


Figure S6. Figure S6. SEM image showing uniform distribution of InAs nanowires on the surface of structural electrolyte GF_PEO-PVP-InAsNW-NaPF₆.

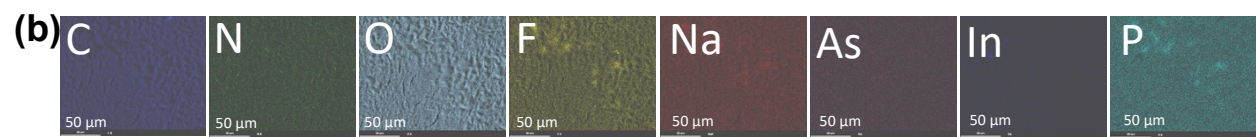
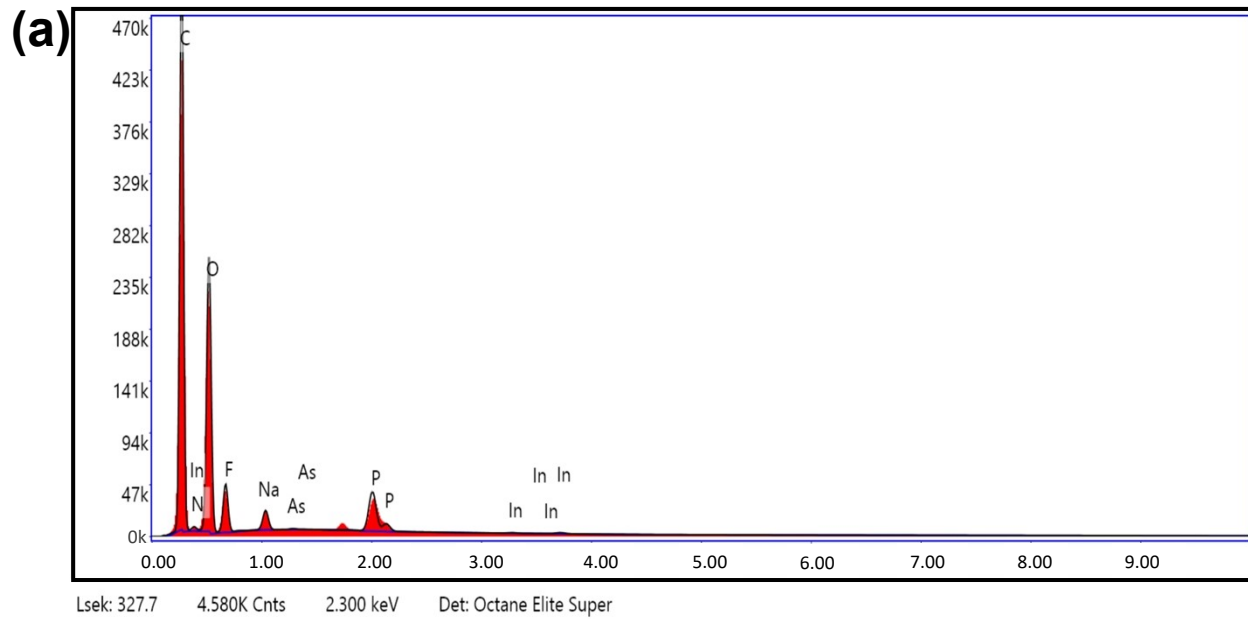


Figure S7. (a) EDAX pattern for the structural electrolyte GF_PEO-PVP-InAsNW-NaPF₆. (b) SEM-EDAX element mapping for the structural electrolyte.

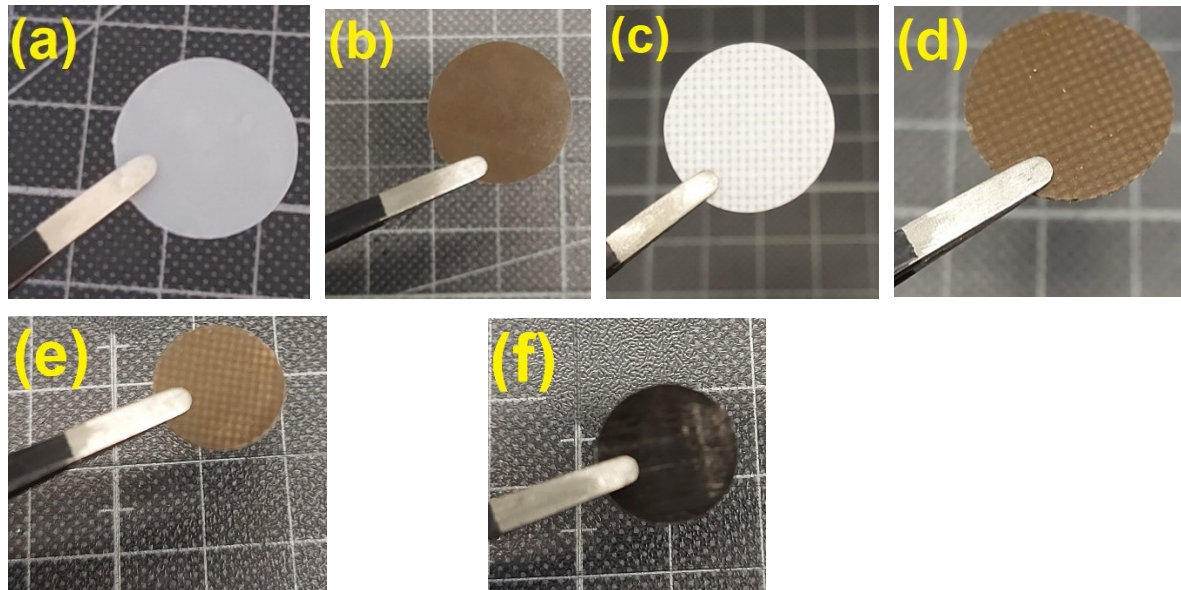


Figure S8. Fabricated electrolytes samples: (a) SPE PEO-PVP-NaPF₆. (b) SPE PEO-PVP-InAsNW-NaPF₆. (c) Structural electrolyte GF_PEO-PVP-NaPF₆. (d) Structural electrolyte GF_PEO-PVP-InAsNW-NaPF₆. (e) Structural electrode upper surface. (f) Structural electrode lower surface showing intermediate carbon fiber electrode

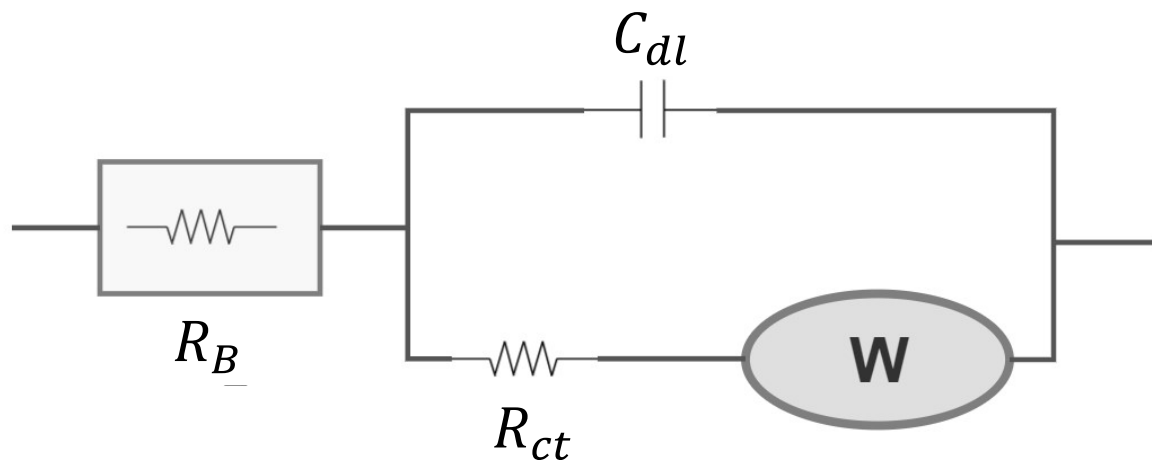


Figure S9. Electrochemical impedance spectroscopy (EIS) equivalent circuit for the electrolytes, with C_{dl} - the double layer interface capacitance, and W – Warburg element representing the solid-state diffusion of Na⁺ into the electrodes.

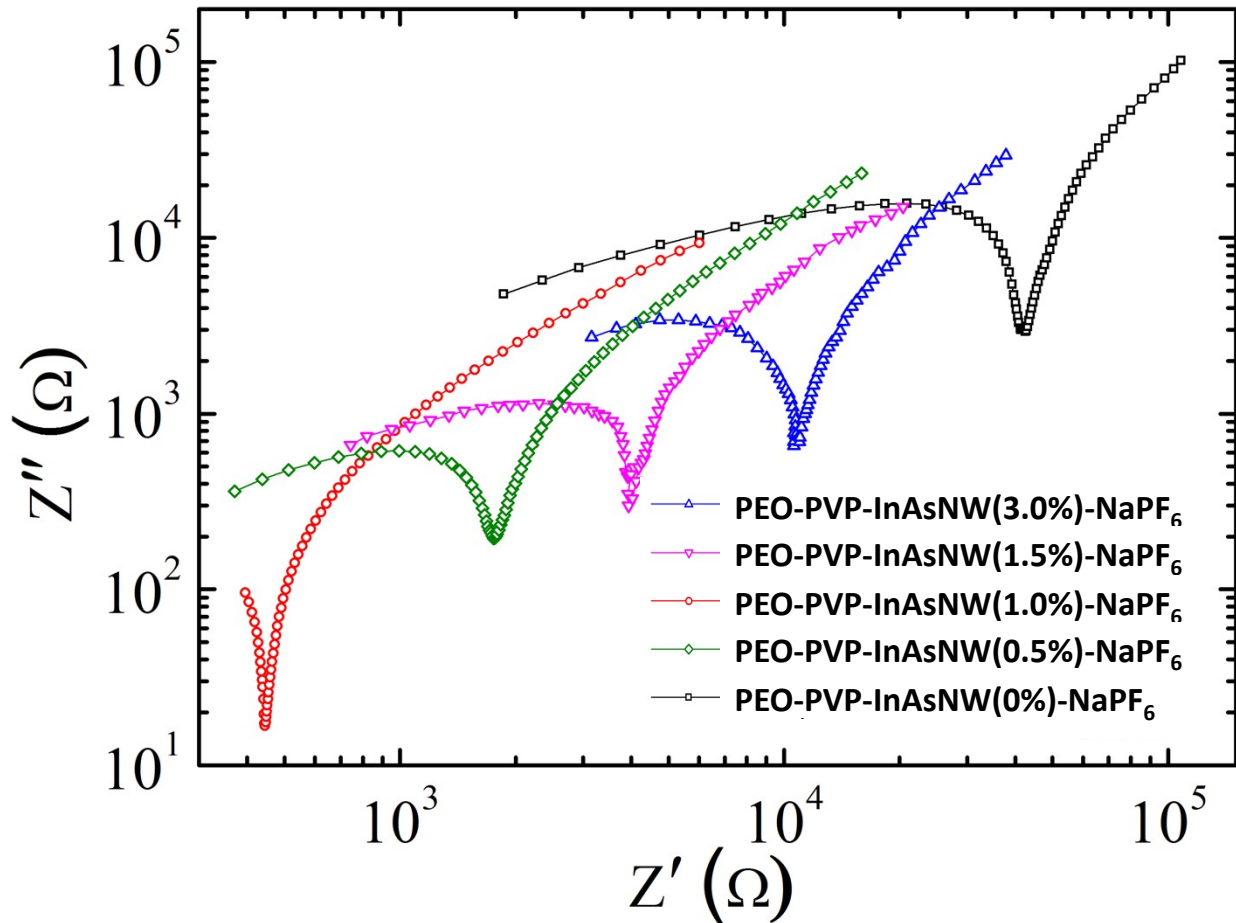


Figure S10. Electrochemical impedance spectroscopy (EIS) spectra of solid polymer electrolytes filled with various amounts of InAs nanowires plotted on double logarithmic scale.³

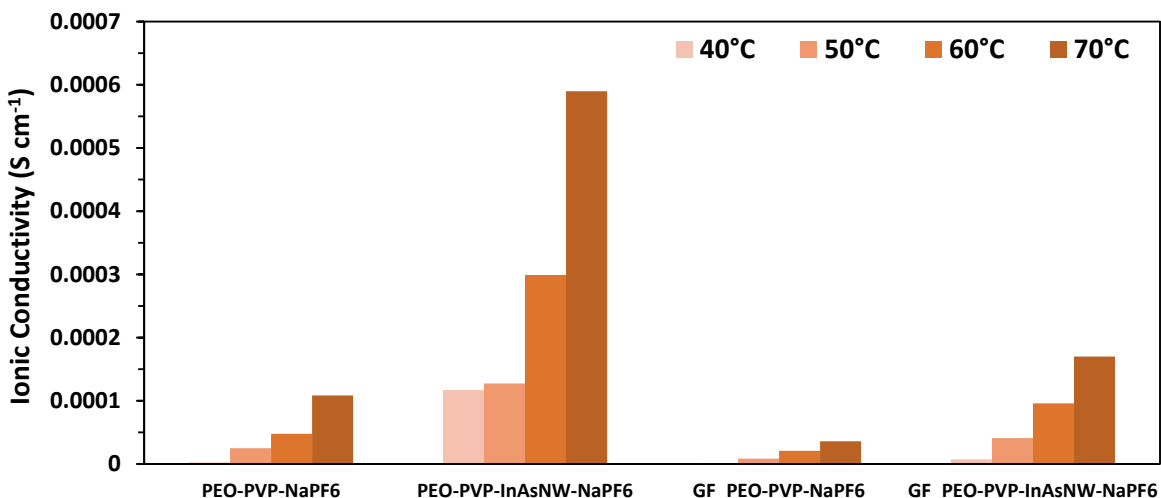


Figure S11. Ionic conductivities of electrolytes at different temperatures.

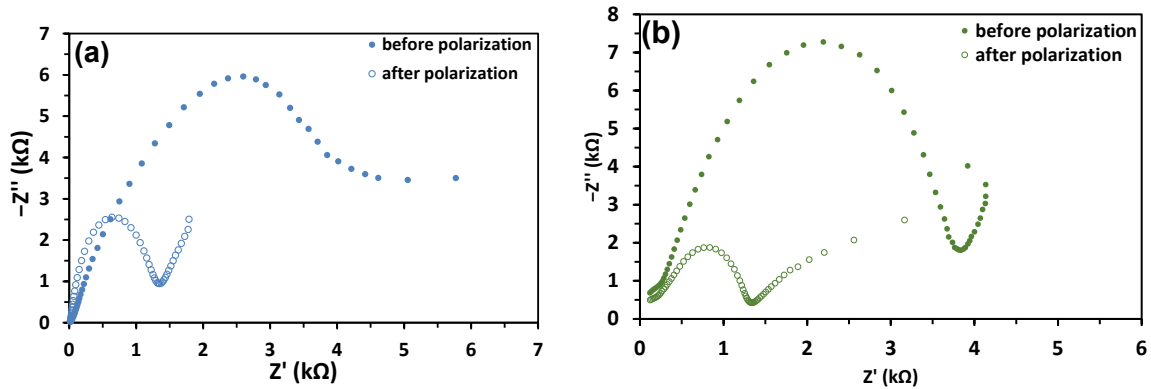


Figure S12. EIS spectra before and after dc polarization for transference-ion measurements: a) Na || PEO-PVP-NaPF₆ || Na. b) Na || GF_PEO-PVP-InAsNW-NaPF₆ || Na.

Table S 1: Sodium-ion transference number calculations

Electrolyte	R ₀ (k Ω)	R _{SS} (k Ω)	Transference ion numbers
PEO-PVP-NaPF ₆	1.04	3.9	0.25
GF_PEO-PVP- InAsNW-NaPF ₆	1.4	3.6	0.40

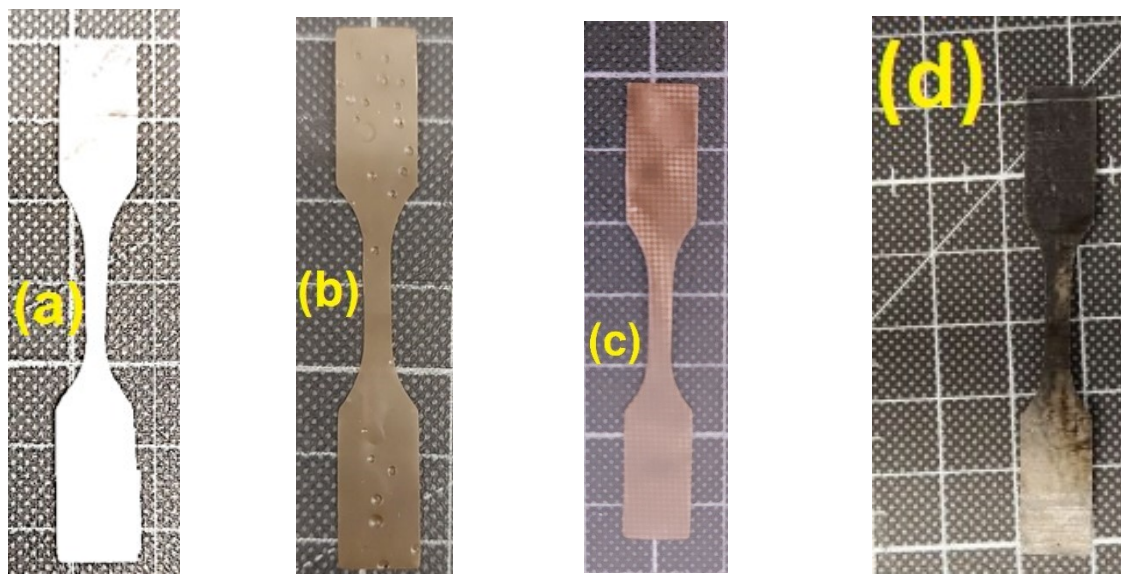


Figure S13. Samples for tensile testing prepared according to ASTM D-638 standards: (a) SPE PEO-PVP-NaPF₆. (b) SPE PEO-PVP-InAsNW-NaPF₆. (c) Structural electrolyte GF_PEO-PVP-InAsNW-NaPF₆. (d) Structural electrode CF | GF_PEO-PVP-InAsNW-NaPF₆.

Table S2: Tensile strength comparison of solid polymer electrolytes

Solid polymer electrolyte (SPE)	Tensile strength (MPa)
PEO-NaClO ₄	0.05 ¹
PEO-NZSP-NaClO ₄	0.15 ¹
PEO-PVP-NaPF ₆ (this work)	4.5
PEO-PVP-InAsNW-NaPF ₆ (this work)	6.1

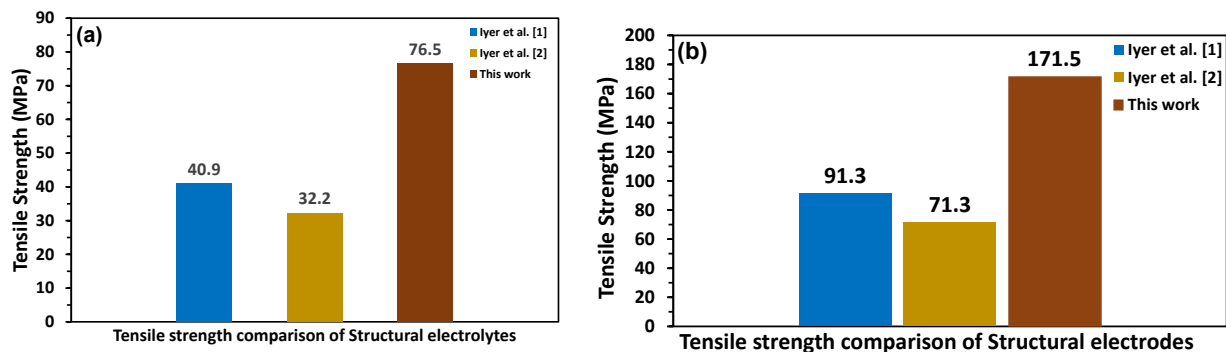


Figure S14. Plot showing comparison of the tensile strength of structural electrolytes for sodium-ion based structural battery.

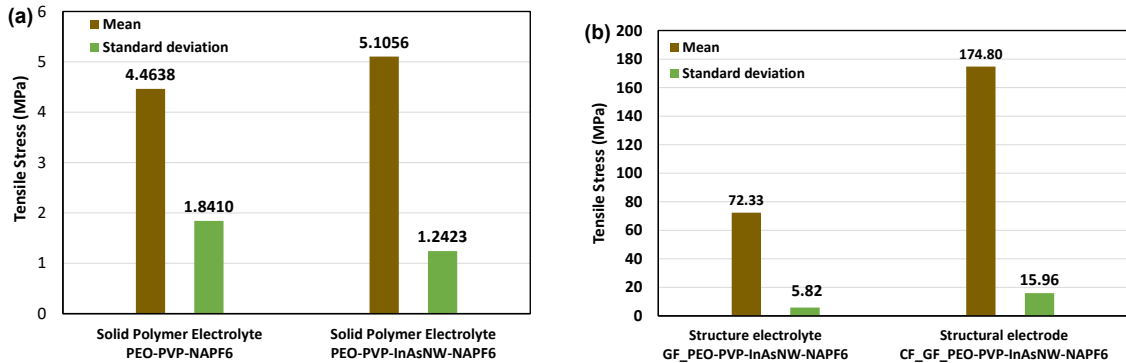


Figure S15. Statistical analysis of tensile tests for: (a) Solid polymer electrolytes. (b) Structural electrolyte and structural electrode.

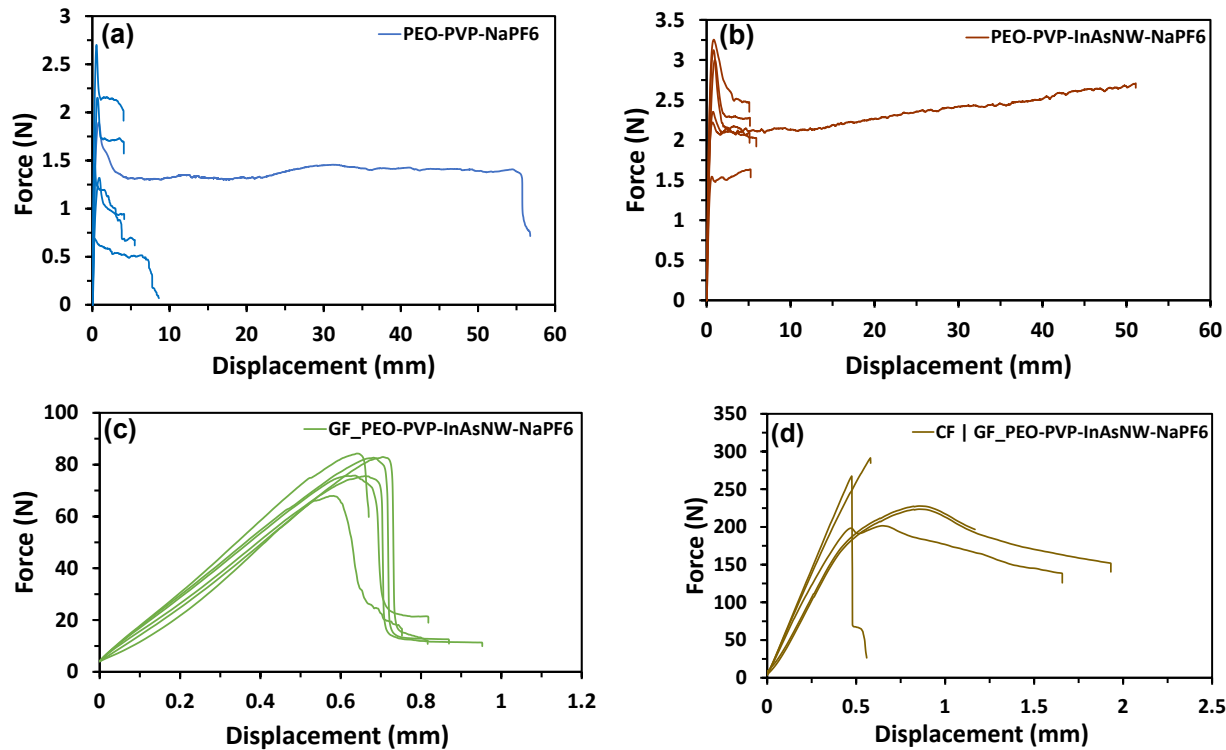


Figure S16. Force – displacement plots from tensile testing: (a) SPE PEO-PVP-NaPF₆. (b) SPE PEO-PVP-InAsNW-NaPF₆. (c) Structural electrolyte GF_PEO-PVP-InAsNW-NaPF₆. (d) Structural electrode CF | GF_PEO-PVP-InAsNW-NaPF₆.

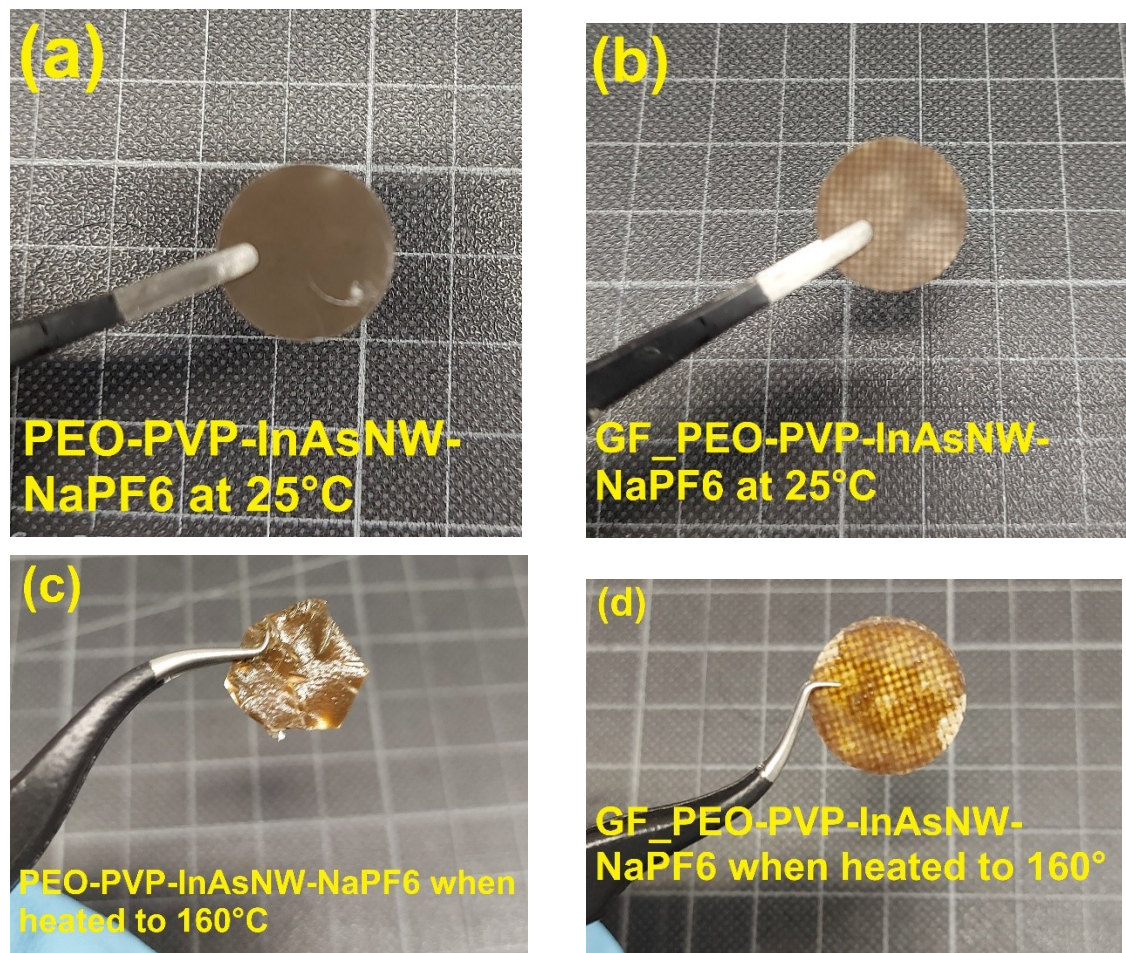


Figure S17. Thermal stability tests: (a) SPE PEO-PVP-InAsNW-NaPF₆ at 25°C. (b) Structural electrolyte GF_PEO-PVP-InAsNW-NaPF₆ at 25°C. (c) SPE PEO-PVP-InAsNW-NaPF₆ after heating to 160°C for 10 minutes. (d) Structural electrolyte GF_PEO-PVP-InAsNW-NaPF₆ after heating to 160°C for 15 minutes.

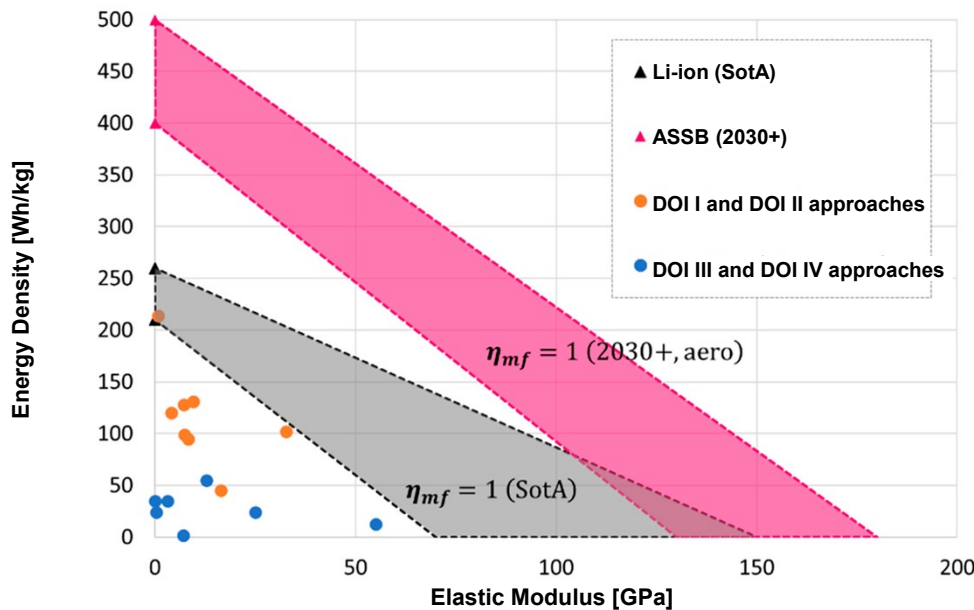


Figure S18. Plot showing comparison of energy density vs elastic modulus for various reported structural batteries in the literature [8, 10]. The plot also indicates the targets for structural batteries for aero applications for the year 2030+ (pink area). The grey area denotes the state-of-the-Art (SotA) for Li-ion batteries. Image reproduced with permission [11].

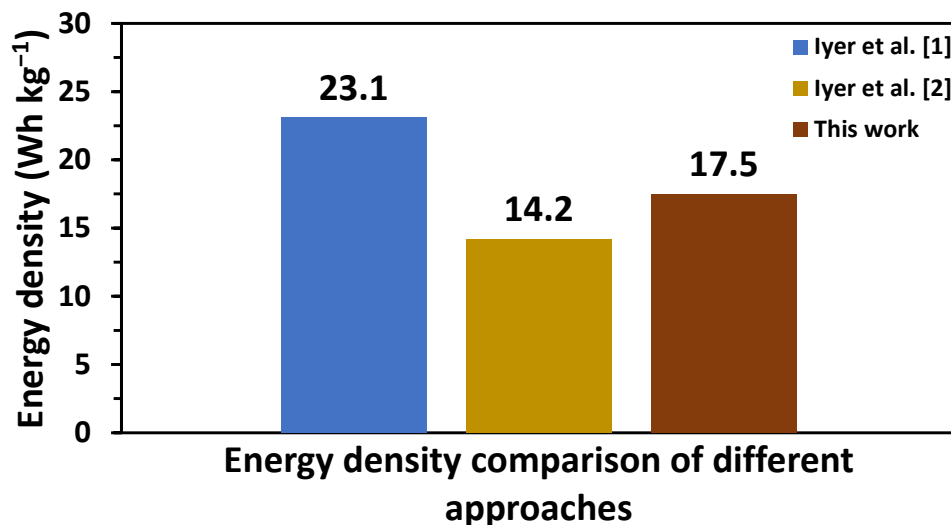


Figure S19. Plot showing comparison of the energy densities reported in different approaches for sodium-ion based structural cell.

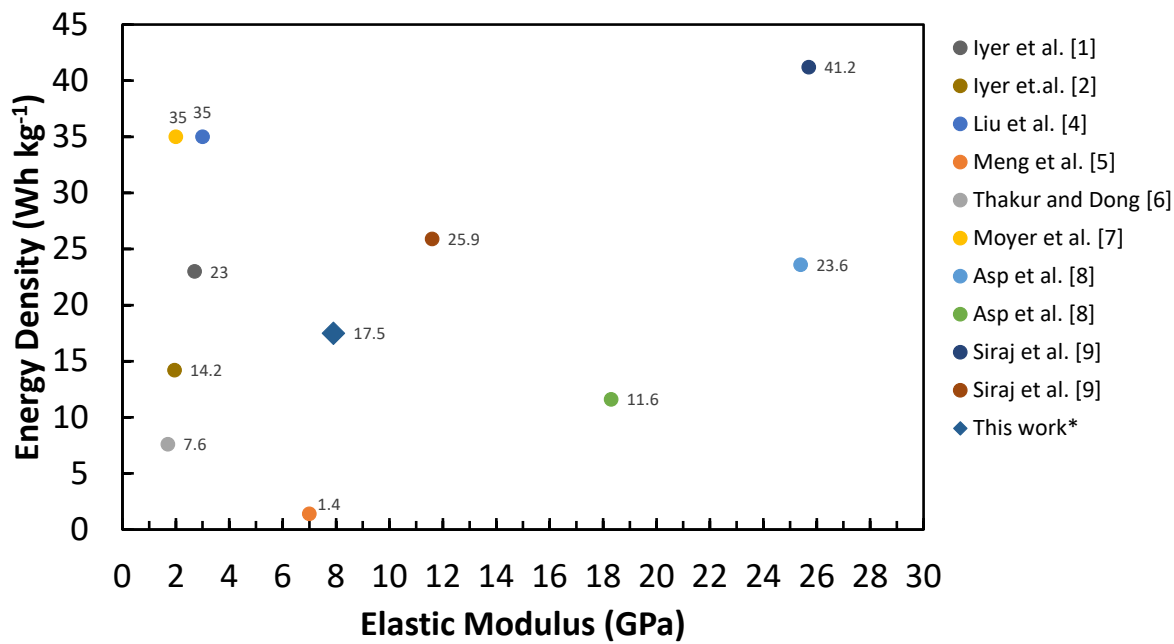


Figure S20. Comparison of energy density vs elastic modulus for DOI III type structural batteries reported in literature.

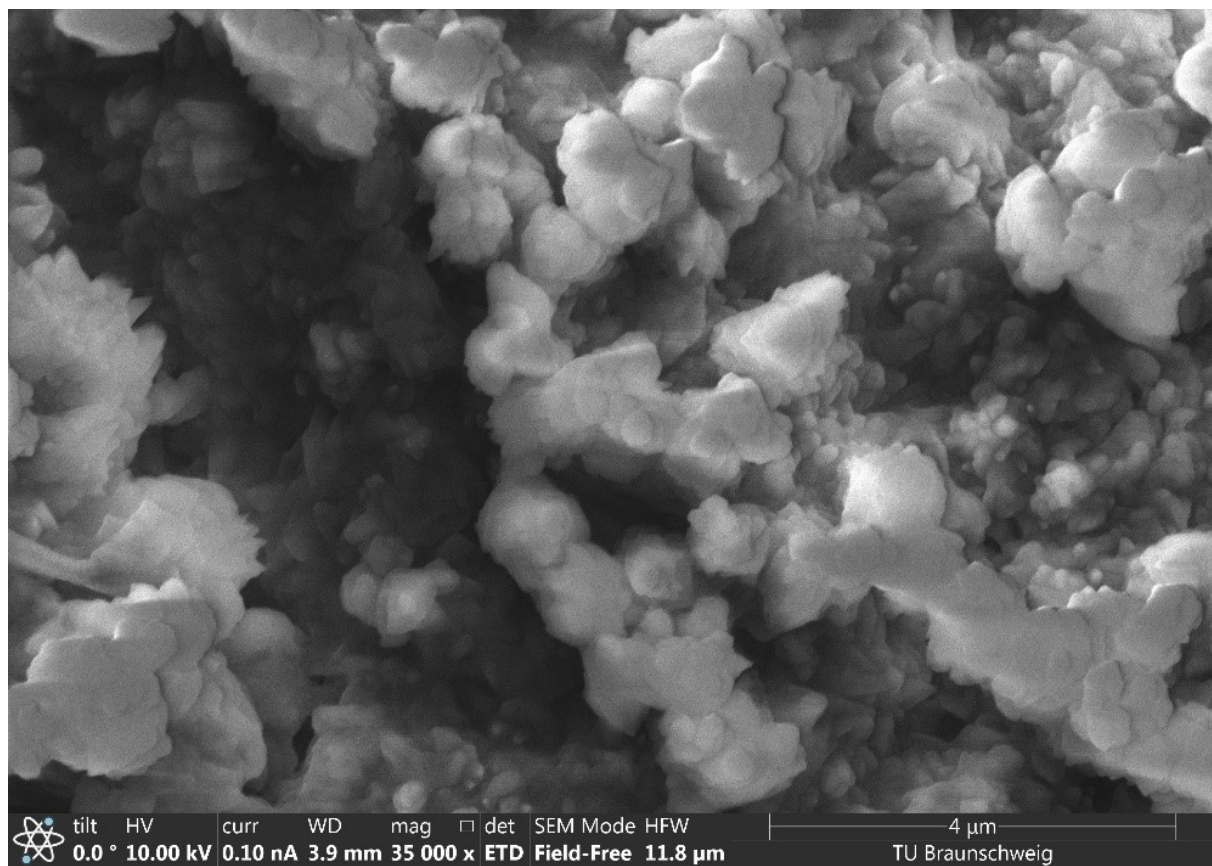


Figure S21. SEM image of Na electrode of the structural cell CF || PEO-PVP-InAsNW-NaPF₆ || Na after cycling.

Table S3. Table showing the performance comparison of various DOI III type structural battery architectures reported in literature

References	Electrolyte type	Structural battery fabrication technique	Ion Type	Reported values		
				C rate	Specific capacity (Ah kg ⁻¹)	Energy density (Wh kg ⁻¹)
Liu et al. ⁴	Gel-polymer type electrolyte	Lamination of carbon fibers to electrolytes	Li ion	0.05C	DNA ^{a)}	35
Meng et al. ⁵	Kevlar reinforced gel type electrolyte	Use of heterogenous materials interfaces using carbon nanotubes	Li ion	DNA ^{a)}	DNA ^{a)}	1.4
Thakur and Dong ⁶	Solid polymer type electrolyte coated on individual carbon fibers	multi-axis coextrusion deposition	Li ion	0.5C	23.4	7.6
Moyer et al. ⁷	Liquid electrolyte impregnated on Celgard separator	Vacuum infusion of electrolyte	Li ion	0.1C	30	35
Asp et.al. ⁸	Bi-continuous phase type electrolyte with GF plain weave separator	Thermal curing after electrolyte impregnation	Li ion	0.05C	8.55	23.6
Asp et.al. ⁸	Bi-continuous phase type electrolyte with Whatman GF /A separator	Thermal curing after electrolyte impregnation	Li ion	0.05C	4.13	11.6
Siraj et.al. ⁹	Bi-continuous phase type electrolyte with GF plain weave separator	Thermal curing after electrolyte impregnation	Li ion	0.05C	14.7	41.2
Siraj et.al. ⁹	Bi-continuous phase type electrolyte with Whatman GF /A separator	Thermal curing after electrolyte impregnation	Li ion	0.05C	9.82	25.9
Iyer et al. ¹	PEO-based SPE incorporated with NZSP nanoparticle fillers, reinforced with glass-fiber separator	Solution casting (Step 1) followed by heat pressing (Step 2) under high pressure and temperature	Na ion	0.1C	10.8	23 ^{b)}
Iyer et al. ²	PEO-based SPE incorporated with succinonitrile plasticizer fillers, reinforced with glass-fiber separator	Solution casting (Step 1) followed by heat pressing (Step 2) under ambient pressure and temperature	Na ion	0.1C	7.5	14.2 ^{b)}
This work	PEO-PVP blend based SPE incorporated with InAs nanowire fillers, reinforced with glass-fiber separator	Solution casting (Step 1) followed by heat pressing (Step 2) under high pressure and temperature	Na ion	0.1C	7.3	17.5 ^{b)}

^{a)}Data Not Available; ^{b)} The energy density values mentioned here are for structural battery half-cells (testing of structural cathode with sodium metal anode).

3. REFERENCES

1. V. Iyer, J. Petersen, S. Geier and P. Wierach, *ACS Appl. Energy Mater.* 2024, **7**, 3968–3982.
2. V. Iyer, J. Petersen, S. Geier and P. Wierach, *Polymers* 2024, **16**, 2806.
3. C. Devi, J. Gellanki, H. Pettersson and S. Kumar, *Sci. Rep.* 2021, **11**, 20180..
4. P. Liu, E. Sherman and A. Jacobsen, *Journal of Power Sources*, 2009, **189**, 646..
5. C. Meng, N. Muralidharan, E. Teblum, K. E. Moyer, G. D. Nessim and C. L. Pint, *Nano Lett.*, 2018, **18**, 7761-7768.
6. A. Thakur and X. Dong, *Manuf. Lett.*, 2020, **24**, 1-5.
7. K. Moyer, C. Meng, B. Marshall, O. Assal, J. Eaves, D. Perez, R. Karkkainen, L. Roberson and C. L. Pint, *Energy Stor. Mater.*, 2020, **24**, 676-681.
8. L. E. Asp, K. Bouton, D. Carlstedt, S. Duan, R. Harnden, W. Johannisson, M. Johansen, M. K. G. Johansson, G. Lindbergh, F. Liu, K. Peuvot, L. M. Schneider, J. Xu and D. Zenkert, *Adv. Energy Sustainability Res.*, 2021, **2**, 2000093
9. M. S. Siraj, S. Tasneem, D. Carlstedt, S. Duan, M. Johansen, C. Larsson, J. Xu, F. Liu, F. Edgren and L. E. Asp, *Adv. Energy Sustainability Res.* 2023, **4**, 2300109.
10. B. J. Hopkins, J. W. Long, D. R. Rolison, J. F. Parker, *Joule* 2020, **4**, 2240–2243.
11. H. Kühnelt, A. Beutl, F. Mastropierro, F. Laurin, S. Willrodt, A. Bismarck, M. Guida and F. Romano, *Aerospace*, 2022, **9**, 7.